3D Multiphysics Modelling of Three-Phase Transformer

Kendeg Onla Clement Junior, Kenmoe Fankem Eric Duckler, Dountio Tchioffo Alix and Effa Joseph Yves

Department of Physics, Faculty of Science, University of Ngaoundere, Cameroon

E-mails : kclementjunior@yahoo.fr, fankeme@yahoo.fr, dountioalix@yahoo.fr, yveseffa@gmail.com

ABSTRACT

Transformers are part of key elements in power distribution or use. With the power of new generation of calculators and development in software engineering, deepen transformers studies is made easier. This paper hence presents a 3D Multiphysics model for temperature prediction of three types of three phase transformer so called Y-shape, 3-columns and 5-culumns transformers. The Finite element method (FEM) is used for the nonlinear calculation of the magnetic field associated with the circuit equations after what a laminar flow model applied to the coolant provides the temperature distribution. Simulation results are obtained from COMSOL Multiphysics software. From them, it is possible to predict the temperature distribution in the transformer. It is also possible to estimate the temperature at specific points that are difficult to reach to perform a measurement and successfully determine the hottest zone inside the transformer.

Keywords: *Computational fluid dynamics (CFD), dry-type transformer, electromagnetic-fluid-thermal analysis method, Multiphysics modelling.*

1. INTRODUCTION

Beyond a certain distance and/or a certain power, the transport of electrical energy must be done under a sufficiently high voltage. To do so, a high voltage level is achieved by the mean of an electrical transformer. It's a static electric machine consisting of two or more coupled windings, with or without a magnetic core to allow mutual coupling between the electrical circuits [1]. The transformer can thus be used to rise up the amplitude of the alternative current (AC) voltage available at the output of the alternator to bring it at the levels required for transport and to reduce it into the values required by the consumers. In [2] and [3] different types of transformers depending on their uses, their cooling modes (submerged and dry-type) or their structures of their magnetic circuits (shell-type, column, triangular and Y-shaped) are presented.

Since transformers are essential components that are used between the supply and the demand (as linker), the harmonic distortions that result from the proliferation of single-phase or three-phase nonlinear loads affect their lifetime [4–8]. Therefore, it becomes imperative to estimate the losses due to those deformations and to study their impacts on the lifetime of the transformers. Several studies have been conducted to analyze, understand and predict the thermal behavior (because of harmonics proliferation) of the transformer for different operating operational states. These works, whether done in 2D or 3D, they use different methods ranging from analytical methods to finite elements. We can cite numerical methods (NT), equivalent circuits method (EC), analytical methods (AM), experimental methods (EM) and hybrid methods (HM). In the Table 1 a summary of the review of the literature about thermal study of the transformer is provided. Else, Fig.1 presents the percentage of study conducted on the thermal modeling of transformers. It can clearly be seen that the electromagnetic-thermal multi-physics and computational fluid dynamics (CFD) studies have the lowest percentage compare to that of other studies. (Thermal Studies (TS), Thermal and Fluidic Studies (TFS), Electromagnetic and Thermal Studies (ETS), Electromagnetic, Thermal and Fluidic Studies (ETFS)).

Table 1. Survey of literature review

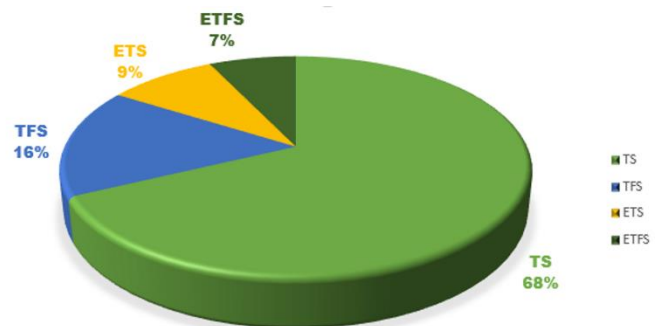| Study	NT	EC	AM	EM	HM
TS	[9-19]	[20-27]	[28-40]	[41-43]	[44–46]
TFS	[47-53]	-	-	-	[54,55]
ETS	[56–59]	-	-	-	[60]
ETFS	[61–64]	-	-	-	-

Fig. 1. Percentage of studies conducted on transformer thermal modeling.

Fig.2 presents the number of different structures encountered in the literature in the 3D modeling of transformers. It can first be noticed that the Y structure has not yet been studied; secondly, the five columns structure also remains very little explored.

The temperature level in the winding and the ferromagnetic circuit of the transformer has a direct influence on its power losses and longevity. This means that the analysis of the physical processes in such equipment is multi physical and should be considered as strongly coupled phenomena.
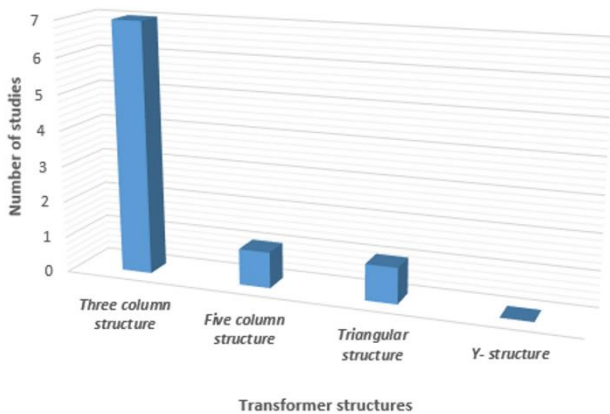
Fig. 2. Percentage of studies conducted on transformer thermal modeling.

Considering all of the above, this paper then steps forwards by proposing a multi physical 3D electromagnetic-thermal and CFD study on three types of structures (five columns, three columns and Y) of transformers. This study also analyses the impact of three load profiles on the primary winding and thus on the power grid. Comsol Multiphysics software is used for simulations and some results are compile in a table to serve as a dashboard for the choice a transformer accordingly to specific requirements. The reminder of this paper is organized as follows. Section 2 describes the different structures studied. Section 3 is dedicated to the principle of Multiphysics modeling of the transformers while section 4 presents the results from simulations. In section 5, the paper is concluded.

2. DEFINITIONS OF THE DIFFERENT STRUCTURES

Three transformer structures classified according to the geometrical shape of the ferromagnetic circuit are considered: the structure in Y, the three columns structure and the five columns structure.

2.1. Geometry of Y shape

A three-phase transformer could be built using three single-phase transformers. However, the total mass of iron and the bulk would be too great. Pooling a core helps reducing the total mass of iron. In a balanced system, the flow through the central iron core is zero since it is the composition of three balanced flows. This iron core is not necessary; this is how we do to get a Y-shaped ferromagnetic circuit (Fig. 3).

2.2. Geometry of the Transformer with Three Columns

Still referred as forced flux flow or forced-flux transformers, they have only three columns and the flow close at least partially in the air through high reluctance paths (Fig. 4).

2.3. Geometry of the Transformer with Five Columns

Still called free-flux transformers, they make it possible to fill more or less considerable failures of the three-column geometry. Here, a fourth or even a fifth column to the magnetic circuit of the transformer is added. These columns channel the flux through a very weak reluctance path. This flux can become

important; it is no longer imposed by the structure of the transformer; the flux can therefore freely move in the ferromagnetic circuit (Fig. 5).
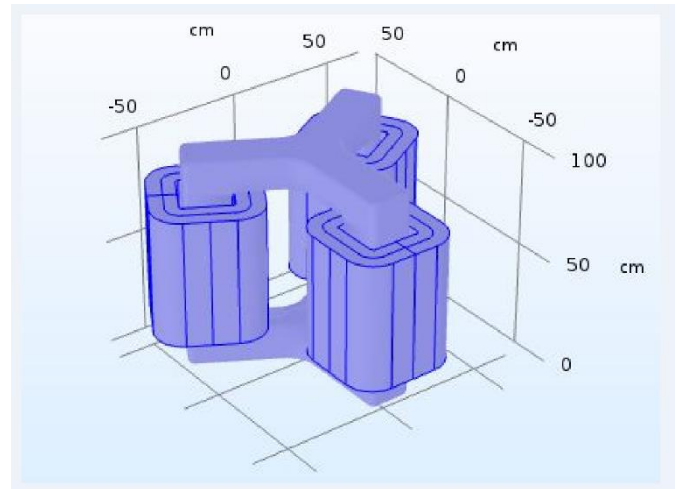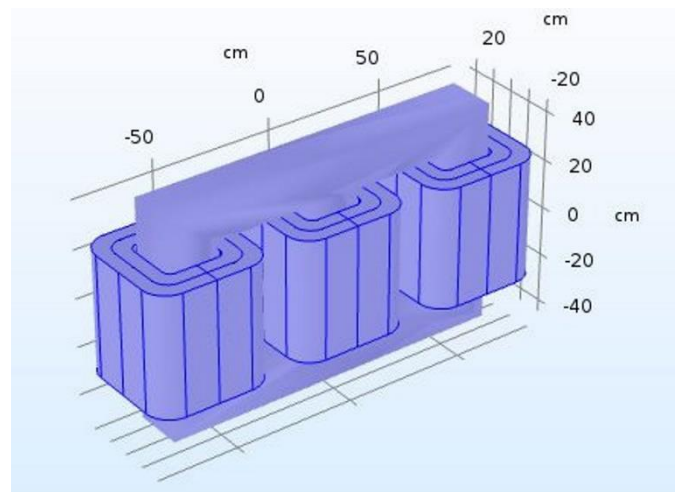

Fig. 3. Y-shaped transformer.

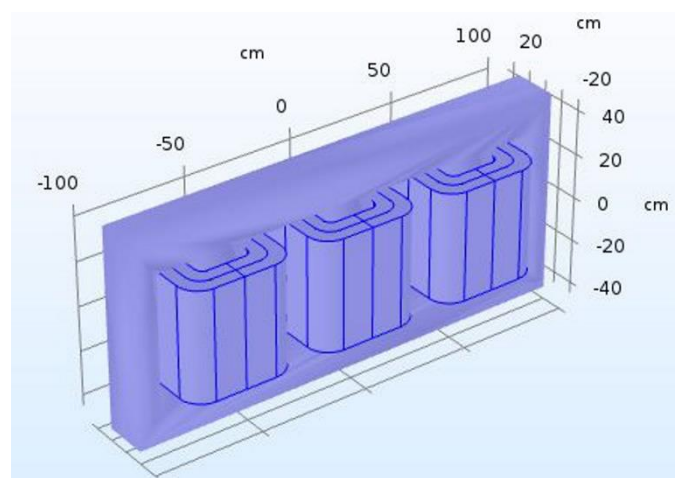**Fig. 4.** Transformer with three columns or forced flow.

Fig. 5. Transformer with five columns or free flow.

3. MULTIPHYSICS MODELLING

3.1. Methodological Approach

The present work uses a 3D finite element method (FEM) for the nonlinear computation of the magnetic field that is associated with the circuit equations. The resulting electromagnetic volume losses are then used as a heat source in the thermal model. The temperature distribution is then obtained by applying a laminar flow model to the cooling fluid. Finally, the multiphysical model obtained is applied to a medium power distribution transformer to evaluate the overheating generated by non-sinusoidal currents. The methodological approach used is summarized in the diagram below (Fig. 6).
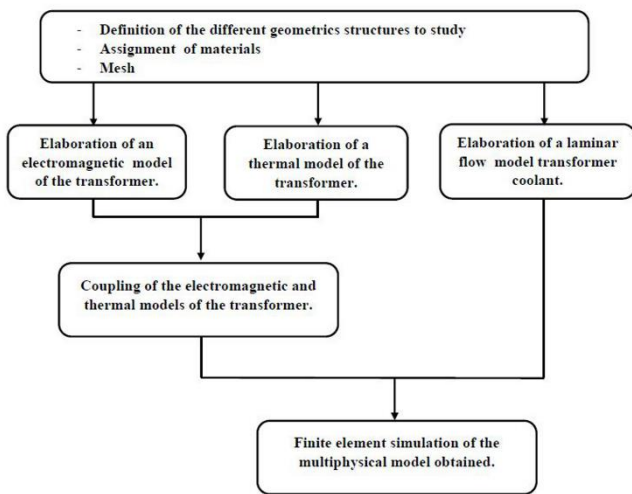

Fig. 6. Diagram of the methodological approach.

3.2. Materials Assignment

The materials used in this modeling are those practically encountered in a transformer; therefore, we obtain three main materials namely: iron (for ferromagnetic circuit), copper (for primary and secondary coils) and air (like cooling fluid).

3.2.1. Iron

The iron considered here is as a ferromagnetic material to model the transformer magnetic circuit whose essential role is to channel the magnetic flux. The Properties of iron are shown in Table 2 and its B-H characteristic curve is presented in Fig. 7. From the last, an optimal use of the material is assured if the magnetic field has a value that is around 1.8 Tesla, but this value should not exceed 1.9 Tesla because beyond this value any increase in the magneto motive force would be unimportant.

3.2.2. Copper

The magnetic flux channeled by the ferromagnetic material defined above is created by turns wound on the magnetic circuit and crossed by a current. The recommended material for the manufacture of the winding of the transformer is copper, whose main characteristics are presented in Table 3.

3.2.3. Air

As far as dry-type transformers are concerned, the cooling fluid used in this work is the air whose presentation of the

different properties is made in Table 4. Expressions of functions and   are respectively given by the relations (1) and (2) [65].

Table 2. Properties of iron

Materials properties	Symbol	Value	Unit
Density	ρ	7850	kg/m^3
Relative Permittivity	ε_r	1	1
Thermal conductivity	k	71.10	$W/(m.K)$
Electrical conductivity	σ	10	S/m
Pressure thermal capacity	C_P	464.57	$J/(kg.K)$

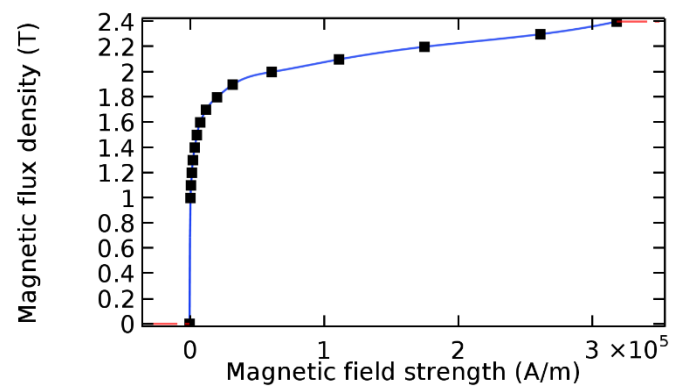**Fig. 7.** Characteristic B-H of the ferromagnetic material.

Table 3. Properties of copper

Materials properties	Symbol	Value	Unit
Density	ρ	8700	kg/m^3
Relative Permittivity	ε_r	1	1
Relative Permeability	μ_r	1	1
Thermal conductivity	k	400	$W/(m.K)$
Electrical conductivity	σ	5.998e7	S/m
Pressure thermal capacity	C_P	385	$J/(kg.K)$

Table 4. Properties of air

Materials properties	Symbol	Value	Unit
Density	ρ	1.23	kg/m^3
Relative Permittivity	ε_r	1	1
Relative Permeability	μ_r	1	1
Thermal conductivity	k	$k(T)$	$W/(m.K)$
Electrical conductivity	σ	10	S/m
Ratio of specific heats	γ	1.4	1
Pressure thermal capacity	C_P	$C_P(T)$	$J/(kg.K)$

$$k(T) = -0.00227583562 + 1.15480022e^{-4} * T^1 -$$
$$7.90252856e^{-8} * T^2 + 4.11702505e^{-11} * T^3 - \quad (1)$$
$$7.43864331e^{-15} * T^4.$$

$$C_P(T) = 1047.63657 - 0.372589265 * T^1 +$$
$$9.45304214e^{-4} * T^2 - 6.02409443e^{-7} * T^3 \quad (2)$$
$$+1.2858961e^{-10} * T^4.$$

3.3. Mesh

Any resolution of a problem by the numerical methods and in particular that of the finite elements must begin by the creation of the mesh representing the field of study. This step is often delicate because the quality of finite element approximation strongly depends on the structure of the mesh.

To carry out our mesh, we used tetrahedrons for the domains (elements in 3D) and triangles for borders (faces or elements in 2D). Fig. 8 to Fig. 12 present the rendering of the mesh made in the frame of our study. We present initially the mesh of the ferromagnetic circuits of the different structures of studied transformer (Fig. 8 to Fig. 10), and then we present the mesh different coils (Fig. 11).
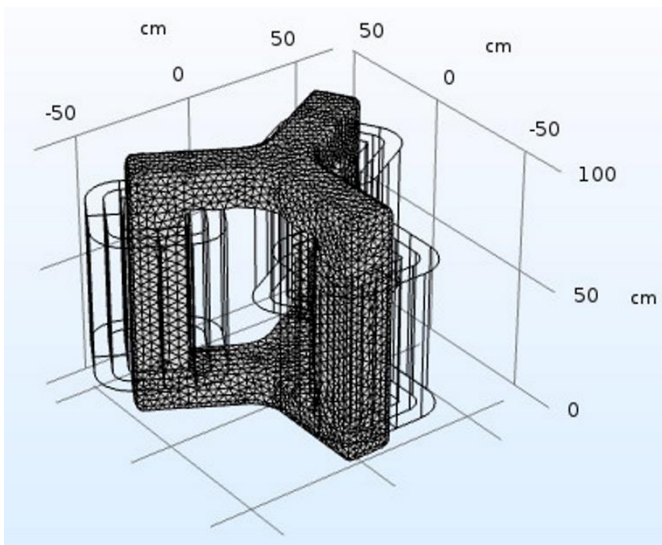

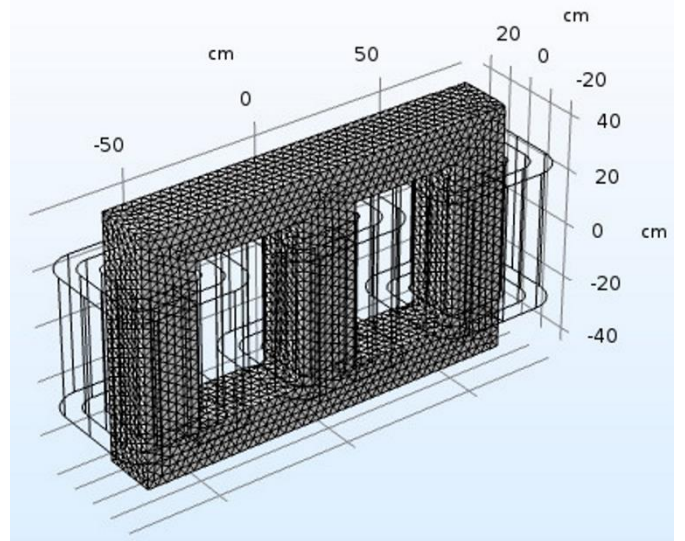**Fig. 8.** Rendering of the mesh of the ferromagnetic circuit in Y.

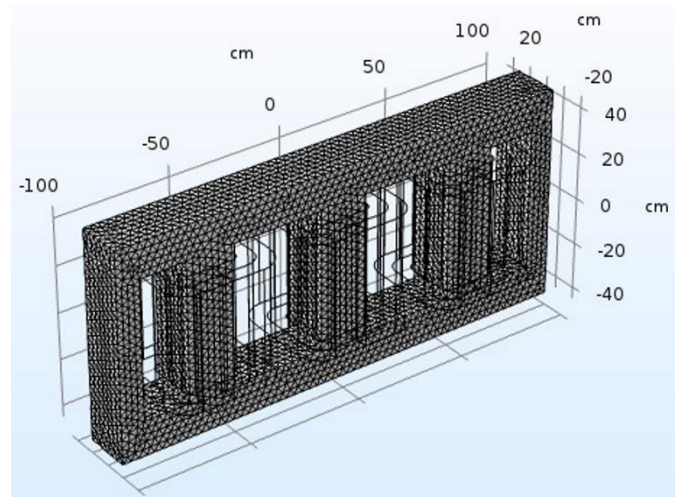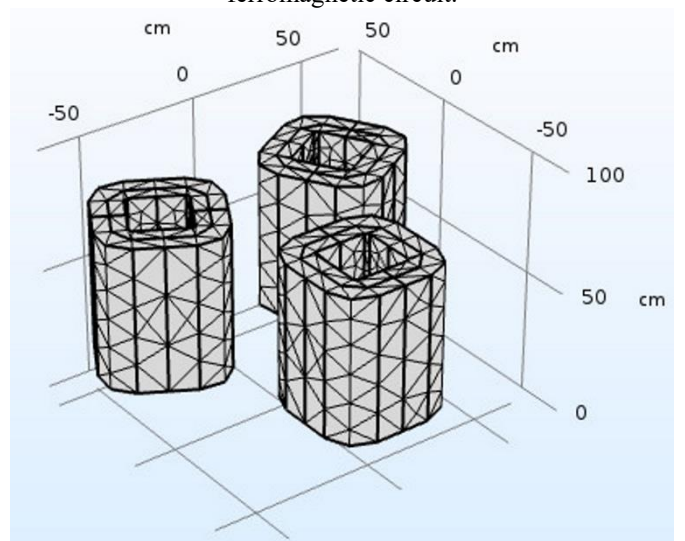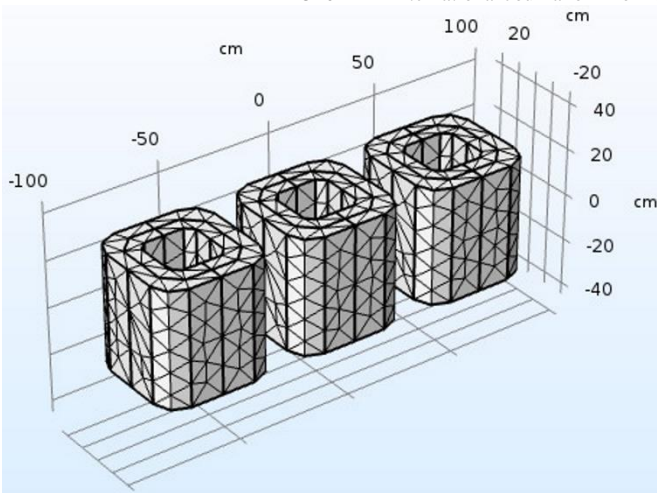**Fig. 9.** Rendering of the mesh of the three-column ferromagnetic circuit.

Fig. 10. Rendering of the mesh of the five-column ferromagnetic circuit.

a. Y structure.

b. Column structure.
Fig. 11. Rendering of the mesh of the primary and secondary winding.

3.4. Electromagnetic modelling

The electromagnetic modeling of the transformer with Comsol involves two modules namely the magnetic field module and the electrical circuit module. The first one is used to calculate the magnetic field and the distribution of the induced current inside and outside the winding of the transformer. To derive the magnetostatic equation, start with Ampère's law for static cases (3). Equation (4) shows the density of current. Using the definitions of magnetic potential (5), the constitutive relationship (6) and equation of Maxwell-Faraday (7), the transient equation of this physics interface solves is Ampère's law (8).

$$\vec{\nabla} \times \vec{H} = \vec{J}. \tag{3}$$

$$\vec{J} = \sigma \vec{v} \times \vec{B} + \vec{J}_e. \tag{4}$$

$$\vec{B} = \vec{\nabla} \times \vec{A}. \tag{5}$$

$$\vec{B} = \mu_0 \left(\vec{H} + \vec{M} \right). \tag{6}$$

$$\vec{E} = -\frac{\partial \vec{A}}{\partial t}. \tag{7}$$

$$\sigma \frac{\partial \vec{A}}{\partial t} + \vec{\nabla} \times \left(\mu_0^{-1} \vec{\nabla} \times \vec{A} - \vec{M} \right) - \sigma \vec{v} \times \left(\vec{\nabla} \times \vec{A} \right) = \vec{J}_e. \tag{8}$$

For the second sub-module, we define three different electrical circuits representing different load profiles (Fig. 12, Fig. 13 and Fig. 14).
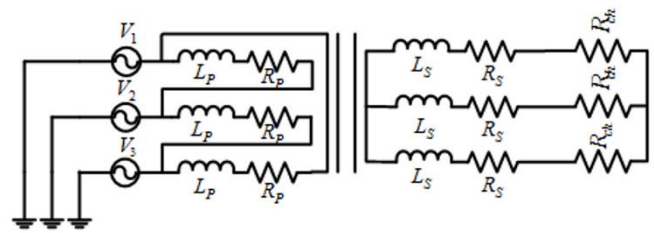

Fig. 12. The dry-type transformer supplies a resistive load (linear load).
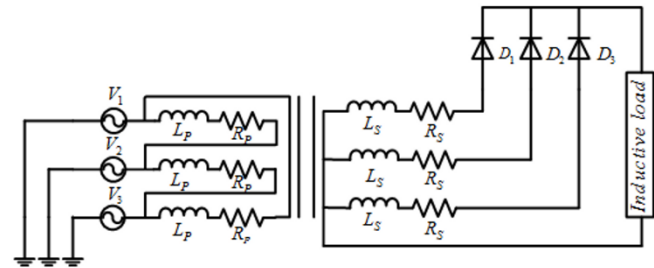

Fig. 13. The dry-type transformer supplies a three-phase half-bridge rectifier with inductive load (nonlinear charge P3).
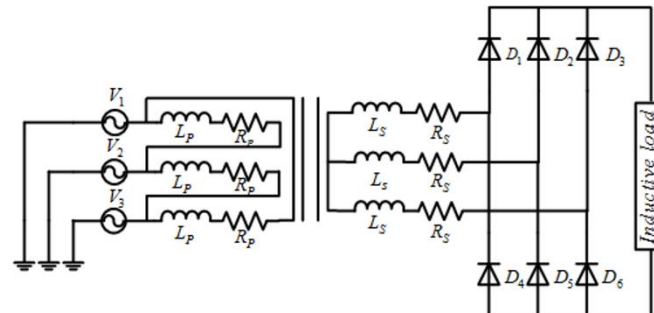

Fig. 14. Transformer supplies a three-phase full-bridge rectifier with inductive load (nonlinear charge PD3).

3.5. Thermal modelling

In this model, the heat source results from electromagnetic volume losses and Joule losses in the primary and secondary winding as these losses are largely responsible for raising the temperature in the transformer tank. Heat transfer in solids and heat transfer in fluids are to be distinguished.

3.5.1. Heat transfer in solids

This interface is used to model the heat transfer in solids by conduction, convection, and radiation. The solved equation is (9).

$$\rho C_p \frac{\partial T}{\partial t} + \vec{\nabla} . \vec{q} = Q. \tag{9}$$

The electromagnetic heating multiphysics coupling adds the source term Q_e to account for resistive heating in the heat equation (9). The thermal conductivity k describes the relationship between the heat flux vector $\vec{q}$ and the temperature gradient $\vec{\nabla} T$ in (10) which is Fourier's law of heat conduction.

ITEE, 10 (2), pp. 33-45, APR 2021   Int. j. inf. technol. electr. eng.

37

$$\vec{q} = -k\vec{\nabla}T \tag{10}$$

Considering all above, equation (9) becomes (11).

$$\rho C_p \frac{\partial T}{\partial t} - \vec{\nabla}.(k\vec{\nabla}T) = Q + Q_e \tag{11}$$

The resistive heating (ohmic heating) due to the electric current is shown by (12).

$$Q_e = \vec{J}.\vec{E} \tag{12}$$

3.5.2. Heat transfer in fluids

This interface is generally used to model the heat transfer by conduction, convection and radiation in fluids. It is used in the present work for the modeling of the heat transfer in the transformer cooling fluid. The relation (13) defines the basic equation retained in this interface.

$$\rho C_p \left(\frac{\partial T}{\partial t} + \vec{u}.\vec{\nabla}T \right) + \vec{\nabla}.(\vec{q} + \vec{q}_r) = Q_p + Q_{vd} + Q. \tag{13}$$

The first term of the right-hand side of (13) is the work done by pressure changes, and is the result of heating under adiabatic compression as well as some thermoacoustic effects. Equation (14) show his expression.

$$Q_p = -\frac{1}{\rho} \frac{\partial \rho}{\partial T} T \left(\frac{\partial p}{\partial t} + \vec{u}.\vec{\nabla}p \right). \tag{14}$$

The second term represents viscous dissipation in the fluid (15).

$$Q_{vd} = \tau : \nabla \vec{u}. \tag{15}$$

It should be noted that the coupling between the electromagnetic model and the thermal model is a strong one. Indeed, the resulting temperature of the thermal model is a parameter of the electromagnetic model, and the density of electromagnetic volume losses and Joule losses resulting from the electromagnetic model are used as the heat source in the thermal model.

3.6. Laminar flow pattern

This interface is used to calculate the velocity and pressure fields for a flow of fluid without phase change and in a laminar flow regime, the Navier- Stokes equations are solve assuming that the flow is incompressible. The equations of motion for a single-phase fluid are the continuity equation (16) and the momentum equation (17).

$$\frac{\partial \rho}{\partial t} + \vec{\nabla}.(\rho \vec{u}) = 0. \tag{16}$$

$$\rho \frac{\partial \vec{u}}{\partial t} + \rho \vec{u}.\vec{\nabla}\vec{u} = -\vec{\nabla}p + \vec{\nabla}.\left[\mu(\vec{\nabla}\vec{u} + (\vec{\nabla}\vec{u})^T) - \frac{2}{3}\mu(\vec{\nabla}.\vec{u})I \right] + \vec{F}. \tag{17}$$

When the temperature variations in the flow are small, a single-phase fluid can often be assumed incompressible; that is, ρ is constant or nearly constant. This is the case for all liquids under normal conditions and for gases at low velocities. In this condition, (16) and (17) becomes (18) and (19) respectively.

$$\rho\vec{\nabla}.\vec{u} = 0. \tag{18}$$

$$\rho \frac{\partial \vec{u}}{\partial t} + \rho(\vec{u}.\vec{\nabla})\vec{u} = \vec{\nabla}.\left[-pI + \mu(\vec{\nabla}\vec{u} + (\vec{\nabla}\vec{u})^T) \right] + \vec{F}. \tag{19}$$

## 4. SIMULATION RESULTS

4.1. Magnetic field cards

The magnetic maps of the Y geometry are shown in Fig. 15. For the case of the linear load (Fig. 15.a) we can see that the maximum density of magnetic flux (B = 1.81 Tesla) is located at the level of the saturation elbow which indicates a good exploitation of the magnetic material employed. With regard to the nonlinear load P3 (Fig. 15.b), we see that the magnetic induction passes at 2.1 Tesla and toggle into the saturation zone of characteristic B(H), hence the ferromagnetic material tick is poorly exploited. The magnetic induction for the nonlinear charge PD3 (Fig. 15.c) has practically the same value as that obtained in the case of a linear load.
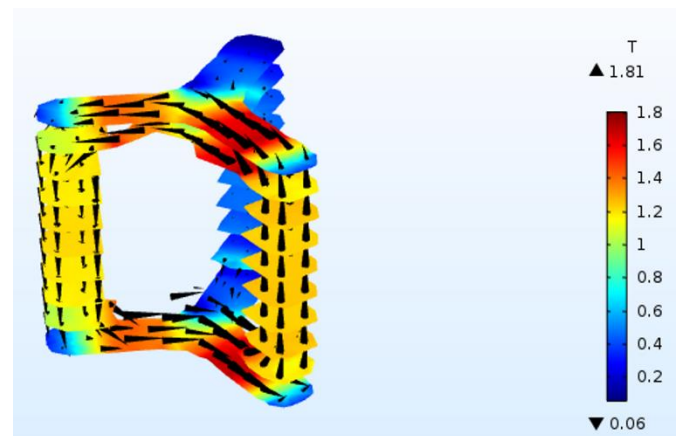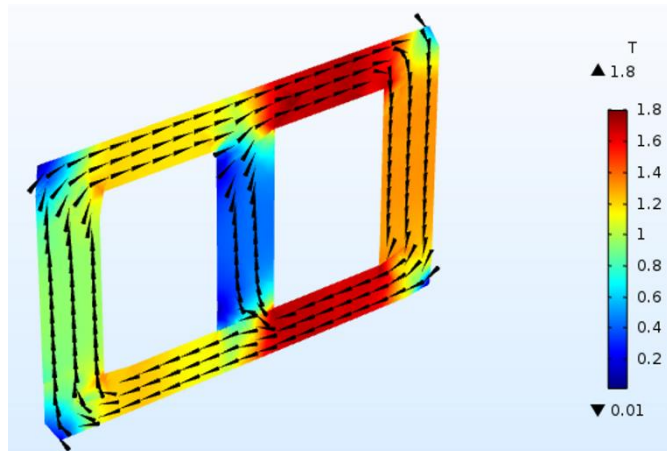

a. case of a linear load.
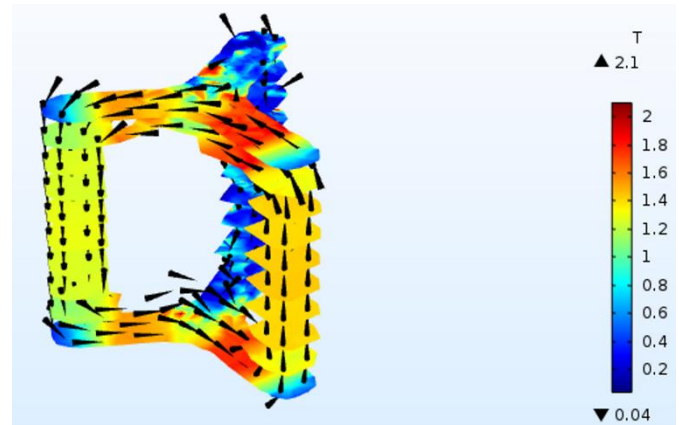
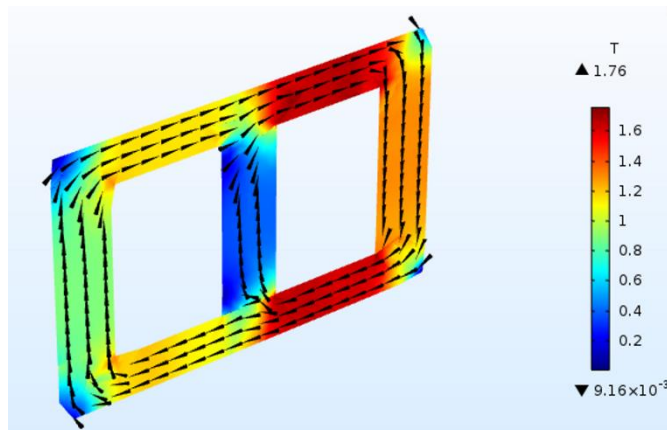

b. case of a nonlinear load P3.
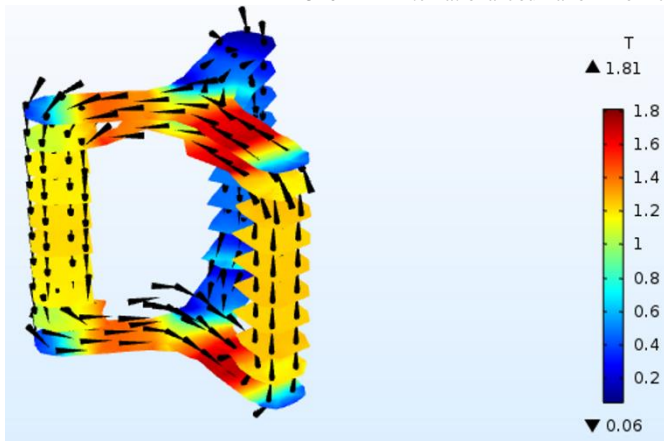
c. case of a nonlinear load PD3.
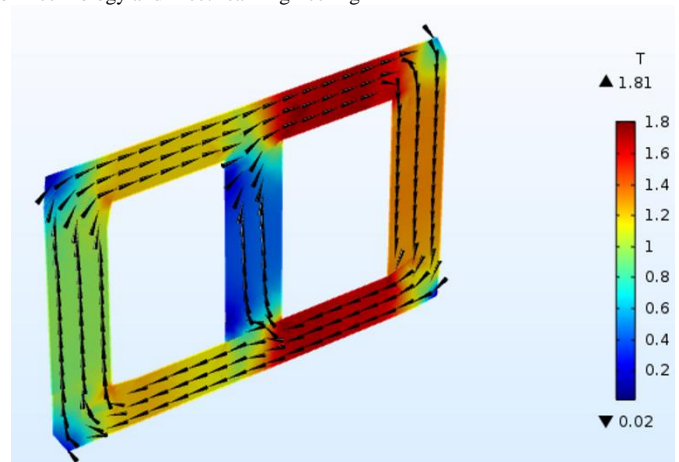**Fig. 15.** Magnetic card of geometry in Y.

Fig. 16 shows the magnetic maps obtained for the three-column geometry; the conclusion is clear. The nature of the load has almost no influence on the density of the magnetic flux in the case of linear load (Fig. 16.a) and the nonlinear load PD3 (Fig. 16.c), because for these two load profiles, the value of the magnetic field is always at the saturation bend. Nevertheless, the nonlinear load P3 has some impact on the density of the magnetic flux. Indeed, considering Fig. 16.b we can observe that the maximum value of magnetic flux density is smaller compared to the two other cases.
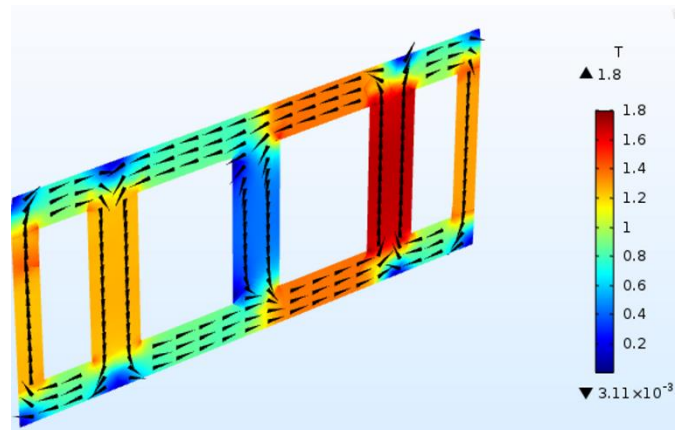

a. case of a linear load.

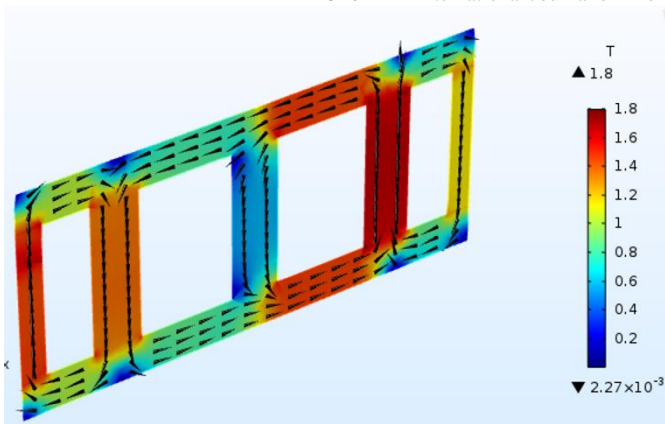**b.** case of a nonlinear load P3.

c. case of a nonlinear load PD3.

Fig. 16. Magnetic card geometry with three columns.

Fig. 17 shows the magnetic maps of the five columns geometry. The observation noted for the three-column geometry remains valid for the case of linear load (Fig. 17.a) and the nonlinear load PD3 (Fig. 17.c). For the case of nonlinear load P3 (Fig. 17.b), we can see that the maximum value of magnetic flux density is same like the two other case. The conclusion is clear; the nature of the load has almost no influence on the density of the magnetic flux because whatever the load profile used the value of the magnetic field is always at the saturation elbow, this transformer structure is more resistant to harmonic disturbances generated by nonlinear loads. This may be due to having two additional flux return columns, which allow the magnetic field lines to move freely in the ferromagnetic circuit.

a. case of a linear load.

b. case of a nonlinear load P3.
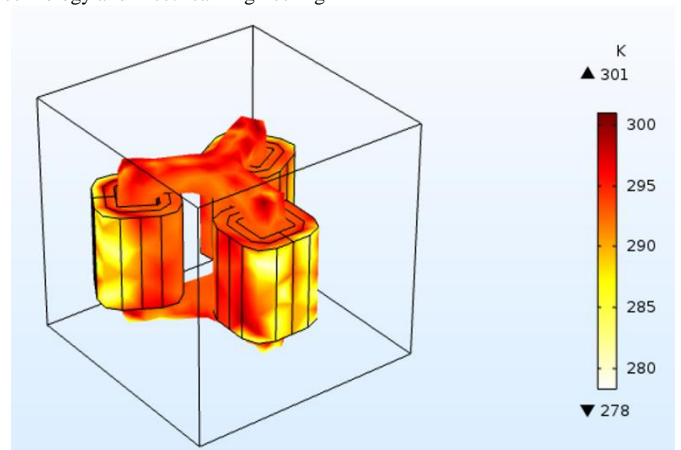
a. case of a linear load.
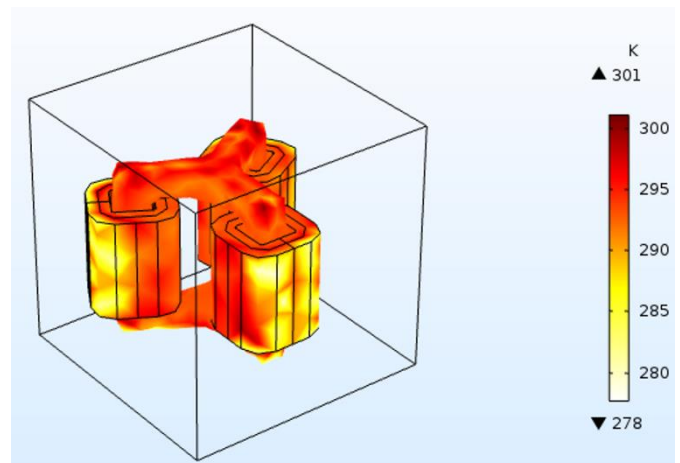
c. case of a nonlinear load PD3.

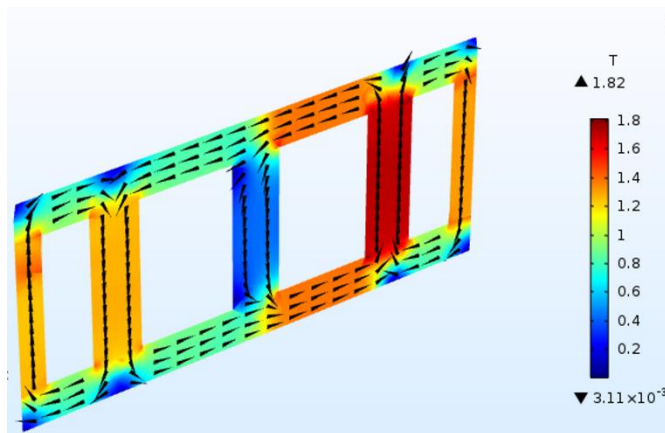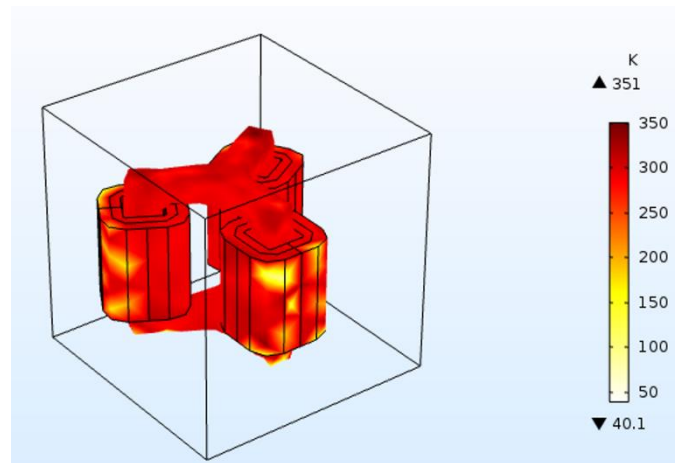**Fig. 17.** Magnetic card geometry with five columns.

b. case of a nonlinear load P3.

4.2. Thermal cards

Transformer thermal maps (ferromagnetic circuit and winding) are presented in Fig. 18 to Fig. 20. Thermal maps of the Y structure (Fig. 18) shows us a temperature rise of about 50K when applying a nonlinear charge P3. For columnar structures, the small rise in temperature is mainly due to the geometric shape of their ferromagnetic circuits, which facilitates heat dissipation and thermal equilibrium. We can also note that, the hot spot of the various transformers is located on the primary winding. This is explained by the fact that they are in contact with the ferromagnetic circuit which is generally at a high temperature, on the other hand the position they occupy which makes their cooling more difficult because the coolant does not access easily, finally in our cases the primary winding is the high voltage winding.
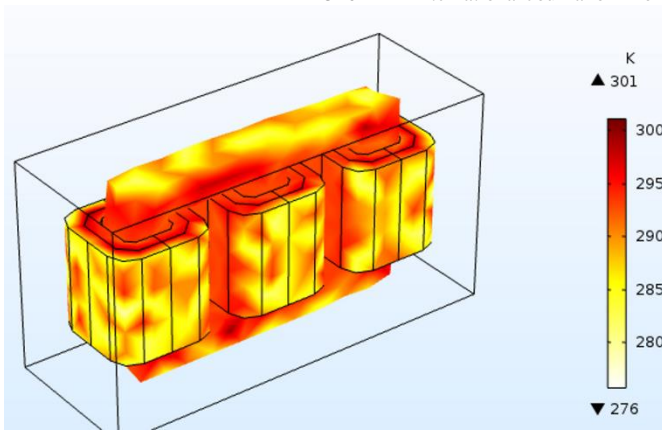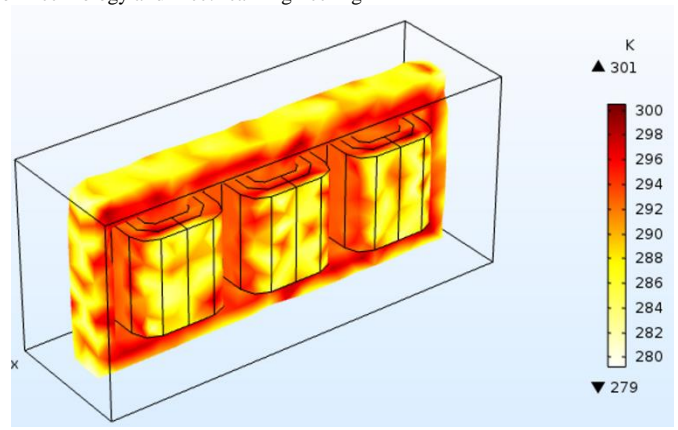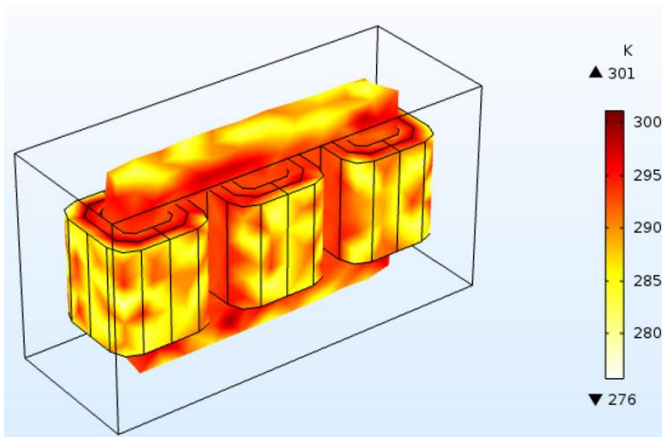
c. case of a nonlinear load PD3

Fig. 18. Transformer thermal card of geometry in Y.

ITEE, 10 (2), pp. 33-45, APR 2021   Int. j. inf. technol. electr. eng.

40
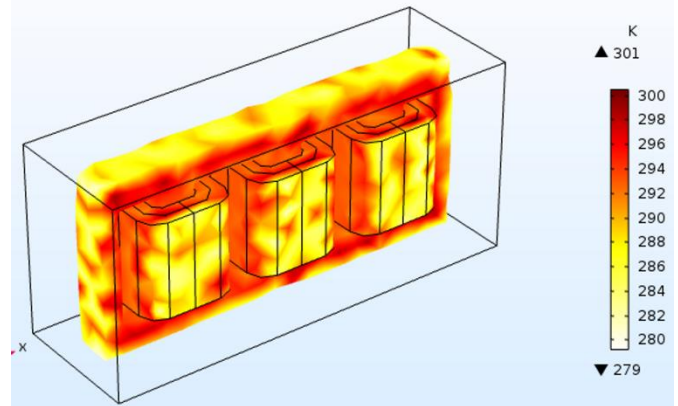
a. case of a linear load.
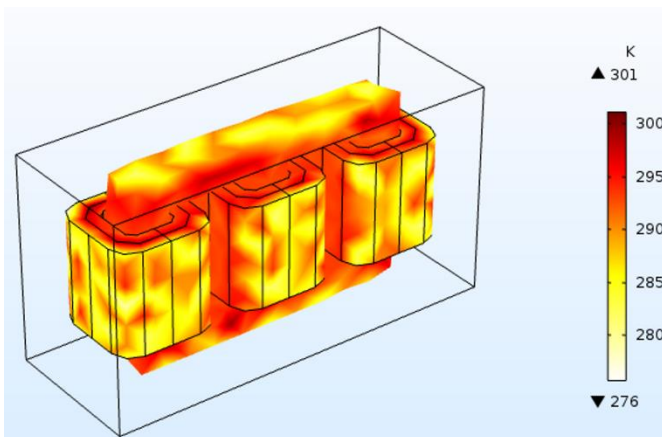
b. case of a nonlinear load P3.
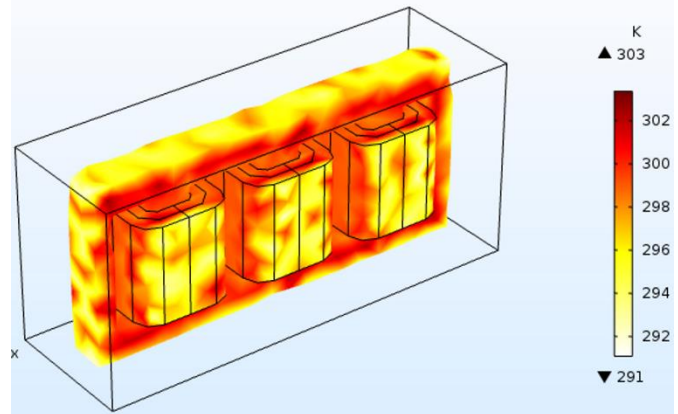
c. case of a nonlinear load PD3.

Fig. 19. Transformer thermal card of geometry with three columns.

a. case of a linear load.

b. case of a nonlinear load P3.

c. case of a nonlinear load PD3.

Fig. 20. Transformer thermal card of geometry with five columns.

In Table 5, a summary of some performances of the structures studied, connected to different types of loads is presented. For harmonics, to assess the performances of the different structures in terms of primary harmonic pollution (injected into the electrical network) by the different charge profiles, we carried out a harmonic analysis passing through the Fourier series decomposition; thereafter we calculated the Total Harmonic Distortion (THD) using relation (20).

$$THD = \sqrt{\frac{\sum_{k=2}^{n} I_k^2}{I_1^2}}. \tag{20}$$

ITEE, 10 (2), pp. 33-45, APR 2021   Int. j. inf. technol. electr. eng.

41

Table 5. Summary comparative Table

	Y-shaped transformer			Three columns			Five columns		
	Linear load	Nonlinear load P3	Nonlinear load PD3	Linear load	Nonlinear load P3	Nonlinear load PD3	Linear load	Nonlinear load P3	Nonlinear load PD3
Harmonics (%)	0.061	7.522	7.495	0.474	47.042	37.290	0.498	76.744	42.748
Temperature (K)	301	351	301	301	301	301	301	301	301
Primary current (A)	600	170	200	1080	160	165	1090	158	148
Magnetic field density (T)	1.810	2.100	1.810	1.800	1.760	1.810	1.800	1.800	1.820
Current density ($10^5 A/m^2$)	8.350	9.510	8.620	2.120	2.390	2.650	2.650	2.920	2.890

With regard to table 5, the Y-shaped structure is very insensitive to harmonics compared to the other two structures. However, it is this same Y structure that has the highest temperature, which can be explained by its complex geometrical shape that does not facilitate the circulation of the cooling fluid. The five-column geometry makes it possible to have an almost constant magnetic flux density whatever the nature of the load, but the harmonics are more pronounced. We can also see that the three-column structure has a lower temperature than the Y structure with a higher harmonic distortion rate (case nonlinear load P3). This same structure compared to that with five columns offers a lower harmonic distortion rate for the three load profiles studied with the same degree of temperature. These two reasons could explain why this transformer structure is more used in the field of distribution of electrical energy.

5. CONCLUSION

In the present paper, a 3D Electromagnetic-thermal-CFD analysis of dry-type transformers is proposed with emphasis on temperature distribution using natural air-cooling. A Comsol Multiphysics based FEM electromagnetic field analysis was first done. Heat source for the thermal-fluid analysis was then obtained and thermal-fluid field analysis based on CFD carried out. Three structures were considered (Y-shape, 3-culumns and 5-culumns) as well as three types of loads (linear and nonlinear loads). Simulations results have helped providing the effects of different loads on those transformers. As expected, the hottest points are found in the primary of the transformers. According to harmonics in the primary winding and the temperature levels, one can find out why the 3-culumns structure is the most used. More, thermal cards can also direct the producers of transformers towards the cooling fins to evacuate as much heat as possible.

6. References:

[1] Transformers Committee, IEEE Power and Energy Society. IEEE Standard Test Code for Dry-Type Distribution and Power Transformers, IEEE Std C57.12.91-2011. 2012.

[2] Amoiralis EI, Tsili MA, Kladas AG. Transformer design and optimization: A literature survey. IEEE Trans Power Deliv 2009. https://doi.org/10.1109/TPWRD.2009.2028763.

[3] Steinmetz T, Smajic J, Outten S, Hartmann T, Carlen M. Benefits of transformers based on triangular wound core configurations. 44th Int. Conf. Large High Volt. Electr. Syst. 2012, 2012.

[4] Dalila MS, Khalid MN, Md Shah M. Distribution transformer losses evaluation under non-linear load.

AUPEC'09 - 19th Australas. Univ. Power Eng. Conf. Sustain. Energy Technol. Syst., 2009.

[5] Salmeron P, Litrán SP. Improvement of the electric power quality using series active and shunt passive filters. IEEE Trans Power Deliv 2010. https://doi.org/10.1109/TPWRD.2009.2034902.

[6] Singh R, Singh A. Aging of distribution transformers due to harmonics. ICHQP 2010 - 14th Int. Conf. Harmon. Qual. Power, 2010. https://doi.org/10.1109/ICHQP.2010.5625347.

[7] Lisita LR, Lima Nerys JW, Batista AJ, de Oliveira AM, Candido Moreira A. Additional Loss in the Core of Three Phase Transformers Feeding Non Linear Loads. IEEE Lat Am Trans 2004. https://doi.org/10.1109/tla.2004.1642379.

[8] Das JC. Power System Harmonics and Passive Filter Designs. 2015. https://doi.org/10.1002/9781118887059.

[9] Pierce LW. Predicting hottest spot temperatures in ventilated dry type transformer windings. IEEE Trans Power Deliv 1994. https://doi.org/10.1109/61.296303.

[10] teNyenhuis EG, Girgis RS, Mechler GF. Calculation of Core Hot-Spot Temperature in Power and Distribution Transformers. IEEE Power Eng Rev 2002. https://doi.org/10.1109/MPER.2002.4312312.

[11] Hwang MD, Grady WM, Wralter HS. Calculation of Winding Temperatures in Distribution Transformers Subjected To Harmonic Currents. IEEE Trans Power Deliv 1988. https://doi.org/10.1109/61.193889.

[12] Eteiba MB, Abdel Aziz MM, Shazly JH. Heat conduction problems in SF6 gas cooled-insulated power transformers solved by the finite-element method. IEEE Trans Power Deliv 2008. https://doi.org/10.1109/TPWRD.2008.915793.

[13] Madžarević V, Kapetanović I, Tešanović M, Kasumović M. Different approach to thermal modeling of transformers-a comparison of methods. Int J Energy Environ 2011;5:610–7.

[14] Barroso R. Simulation and Experimental Validation of the Core Temperature Distribution of a Three-Phase Transformer. Proc. 2014 COMSOL Conf. Curitiba, 2014.

[15] Salari M, Bayrasy P, Wolf K. Thermal analysis of a three phase transformer with coupled simulation. URL Https//Www Res Net/Publication/276 2018;57920.

[16] Mechkov E, Tzeneva R, Mateev V, Yatchev I. Thermal analysis using 3D FEM model of oil-immersed distribution transformer. 2016 19th Int. Symp. Electr. Appar. Technol. SIELA 2016, 2016. https://doi.org/10.1109/SIELA.2016.7543027.

[17] Garelli L, Ríos Rodriguez G, Storti M, Granata D, Amadei M, Rossetti M. Reduced model for the thermo-fluid dynamic analysis of a power transformer radiator working in ONAF mode. Appl Therm Eng 2017. https://doi.org/10.1016/j.applthermaleng.2017.06.098.

[18] Mafra RG, Dos Santos Magalhães E, De Campos Salles Anselmo B, Belchior FN, Lima e Silva SMM. Winding hottest-spot temperature analysis in dry-type transformer

ITEE, 10 (2), pp. 33-45, APR 2021   Int. j. inf. technol. electr. eng.

42

using numerical simulation. Energies 2019. https://doi.org/10.3390/en12010068.

[19] Das AK, Chatterjee S. Finite element method-based modelling of flow rate and temperature distribution in an oil-filled disc-type winding transformer using COMSOL multiphysics. IET Electr Power Appl 2017. https://doi.org/10.1049/iet-epa.2016.0446.

[20] Ryder SA, Vaughan IJ. A simple method for calculating core temperature rise in power transformers. IEEE Trans Power Deliv 2004. https://doi.org/10.1109/TPWRD.2003.820222.

[21] Swift G, Molinski TS, Lehn W. A fundamental approach to transformer thermal modeling - Part I: Theory and equivalent circuit. IEEE Trans Power Deliv 2001. https://doi.org/10.1109/61.915478.

[22] Swift G, Molinski TS, Bray R, Menzies R. A fundamental approach to transformer thermal modeling - Part II: Field verification. IEEE Trans Power Deliv 2001. https://doi.org/10.1109/61.915479.

[23] Radakovic Z, Feser K. A new method for the calculation of the hot-spot temperature in power transformers with ONAN cooling. IEEE Trans Power Deliv 2003. https://doi.org/10.1109/TPWRD.2003.817740.

[24] Susa D, Lehtonen M, Nordman H. Dynamic thermal modelling of power transformers. IEEE Trans Power Deliv 2005. https://doi.org/10.1109/TPWRD.2004.835255.

[25] Mao X, Tylavsky DJ, McCulla GA. Assessing the reliability of linear dynamic transformer thermal modelling. IEE Proc Gener Transm Distrib 2006. https://doi.org/10.1049/ip-gtd:20050172.

[26] Susa D, Lehtonen M. Dynamic thermal modeling of power transformers: Further development - Part II. IEEE Trans Power Deliv 2006. https://doi.org/10.1109/TPWRD.2005.864068.

[27] Susa D, Lehtonen M. Dynamic thermal modeling of power transformers: Further development - Part I. IEEE Trans Power Deliv 2006. https://doi.org/10.1109/TPWRD.2005.864069.

[28] Pradhan MK, Ramu TS. Prediction of hottest spot temperature (HST) in power and station transformers. IEEE Trans Power Deliv 2003. https://doi.org/10.1109/TPWRD.2003.817739.

[29] Rose SB, Ragasudha J. A NEW THERMAL MODELING OF DRY TYPE TRANSFORMERS AND ESTIMATING TEMPERATURE RISE n.d.

[30] Pradhan MK, Ramu TS. Estimation of the hottest spot temperature (HST) in power transformers considering thermal inhomogeniety of the windings. IEEE Trans Power Deliv 2004. https://doi.org/10.1109/TPWRD.2004.835291.

[31] Pradhan MK, Ramu TS. On the estimation of elapsed life of oil-immersed power transformers. IEEE Trans Power Deliv 2005. https://doi.org/10.1109/TPWRD.2005.848663.

[32] Jardini JA, Pereira Brittes JL, Magrini LC, Bini MA, Yasuoka J. Power transformer temperature evaluation for overloading conditions. IEEE Trans Power Deliv 2005. https://doi.org/10.1109/TPWRD.2004.835433.

[33] Susa D, Palola J, Lehtonen M, Hyvärinen M. Temperature rises in an OFAF transformer at OFAN cooling mode in service. IEEE Trans Power Deliv 2005. https://doi.org/10.1109/TPWRD.2005.852284.

[34] Nordman H, Rafsback N, Susa D. Temperature responses to step changes in the load current of power transformers. IEEE Trans Power Deliv 2003. https://doi.org/10.1109/TPWRD.2003.817516.

[35] Ryder S. A Simple Method for Calculating Winding Temperature Gradient in Power Transformers. IEEE Power Eng Rev 2002. https://doi.org/10.1109/MPER.2002.4312309.

[36] Stahlhut JW, Heydt GT, Selover NJ. A preliminary assessment of the impact of ambient temperature rise on distribution transformer loss of life. IEEE Trans Power Deliv 2008. https://doi.org/10.1109/TPWRD.2008.2002848.

[37] Jauregui-Rivera L, Tylavsky DJ. Acceptability of four transformer top-oil thermal models-part I: Defining metrics. IEEE Trans Power Deliv 2008. https://doi.org/10.1109/TPWRD.2007.905555.

[38] Jauregui-Rivera L, Tylavsky DJ. Acceptability of four transformer top-oil thermal models - Part II: Comparing metrics. IEEE Trans Power Deliv 2008. https://doi.org/10.1109/TPWRD.2007.905576.

[39] Lachman MF, Griffin PJ, Walter W, Wilson A. Real-time dynamic loading and thermal diagnostic of power transformers. IEEE Trans Power Deliv 2003. https://doi.org/10.1109/TPWRD.2002.803724.

[40] Akbari A, Allahbakhshi M, Golpari R. Application of interactive multiple models in thermal modeling of power transformers. Eur Trans Electr Power 2011. https://doi.org/10.1002/etep.560.

[41] Pierce LW. An investigation of the thermal performance of an oil filled transformer winding. IEEE Trans Power Deliv 1992. https://doi.org/10.1109/61.141852.

[42] Pierce LW. An investigation of the temperature distribution in cast-resin transformer windings. IEEE Trans Power Deliv 1992. https://doi.org/10.1109/61.127099.

[43] Tylavsky DJ, Mao X, McCulla GA. Transformer thermal modeling: Improving reliability using data quality control. IEEE Trans Power Deliv 2006. https://doi.org/10.1109/TPWRD.2005.864039.

[44] Tsili MA, Kladas AG, Georgilakis PS, Souflaris AT, Pitsilis CP, Bakopoulos JA, et al. Hybrid numerical techniques for power transformer modeling: A comparative analysis validated by measurements. IEEE Trans. Magn., 2004. https://doi.org/10.1109/TMAG.2004.825303.

[45] Silva DCL, Sousa RH, Lima FKA, Branco CGC. Contributions to the study of energy efficiency in dry-type transformer under nonlinear load. IEEE Int. Symp. Ind. Electron., 2015. https://doi.org/10.1109/ISIE.2015.7281511.

[46] Torin LR, Medina DOG, Sousa T. Dry-Type Power Transformers Thermal Analysis with Finite Element Method. Int J Adv Eng Res Sci 2019. https://doi.org/10.22161/ijaers.6.3.19.

[47] El Wakil N, Chereches N-C, Padet J. Numerical study of heat transfer and fluid flow in a power transformer A preliminary version of the paper was presented at CHT-4: An ICHMT International Symposium on Advances in Computational Heat Transfer, April 2004, G. de Vahl Davis and E. Leonardi (E. Int J Therm Sci 2006;45:615–26. https://doi.org/https://doi.org/10.1016/j.ijthermalsci.2005.09.002.

[48] Mufuta JM, Van Den Bulck E. Modelling of the mixed convection in the windings of a disc-type power transformer. Appl Therm Eng 2000. https://doi.org/10.1016/S1359-4311(99)00034-4.

[49] Smolka J, Nowak AJ, Wrobel LC. Numerical modelling of thermal processes in an electrical transformer dipped into polymerised resin by using commercial CFD package fluent. Comput Fluids 2004. https://doi.org/10.1016/j.compfluid.2003.06.008.

[50] Smolka J, Ingham DB, Elliott L, Nowak AJ. Enhanced numerical model of performance of an encapsulated three-phase transformer in laboratory environment. Appl Therm Eng 2007. https://doi.org/10.1016/j.applthermaleng.2006.05.008.

[51] Tsili MA, Amoiralis EI, Kladas AG, Souflaris AT. Power transformer thermal analysis by using an advanced coupled 3D heat transfer and fluid flow FEM model. Int J Therm Sci 2012. https://doi.org/10.1016/j.ijthermalsci.2011.10.010.

[52] Zhang YB, Xin YL, Qian T, Lin X, Tang WH, Wu QH. 2-D coupled fluid-thermal analysis of oil-immersed power transformers based on finite element method. IEEE PES Innov. Smart Grid Technol. Conf. Eur., 2016. https://doi.org/10.1109/ISGT-Asia.2016.7796532.

[53] Liu G, Zheng Z, Yuan D, Li L, Wu W. Simulation of fluid-thermal field in oil-immersed transformer winding based on dimensionless least-squares and upwind finite element method. Energies 2018. https://doi.org/10.3390/en11092357.

[54] Rodriguez GR, Garelli L, Storti M, Granata D, Amadei M, Rossetti M. Numerical and experimental thermo-fluid dynamic analysis of a power transformer working in ONAN mode. Appl Therm Eng 2017. https://doi.org/10.1016/j.applthermaleng.2016.08.171.

[55] Schmidt N, Tenbohlen S, Chen S, Breuer C. Numerical and experimental investigation of the temperature distribution inside oil-cooled transformer windings. Proc. 18th Int. Symp. High Volt. Eng., 2013, p. 25–30.

[56] Preis K, Bíró O, Buchgraber G, Tičar I. Thermal-electromagnetic coupling in the finite-element simulation of power transformers. IEEE Trans. Magn., 2006. https://doi.org/10.1109/TMAG.2006.871439.

[57] Hwang CC, Tang PH, Jiang YH. Thermal analysis of high-frequency transformers using finite elements coupled with temperature rise method. IEE Proc Electr Power Appl 2005. https://doi.org/10.1049/ip-epa:20045247.

[58] Ag ABB, Deutschland F. Transient Electromagnetic-Thermal FE-Model of a SPICE-Coupled Transformer Including Eddy Currents with COMSOL Multiphysics 4. 2. Components 2011. https://doi.org/10.1016/0040-6090(95)06757-4.

[59] Behjat V. A Coupled Thermal-Electromagnetic FEM Model to Characterize the Thermal Behavior of Power Transformers Damaged By Short Circuit Faults. Int J Electr Energy 2013. https://doi.org/10.12720/ijoee.1.4.194-200.

[60] Lefèvre A, Miègeville L, Fouladgar J, Olivier G. 3-D computation of transformers overheating under nonlinear loads. IEEE Trans. Magn., 2005. https://doi.org/10.1109/TMAG.2005.845049.

[61] Smolka J, Nowak AJ. Experimental validation of the coupled fluid flow, heat transfer and electromagnetic numerical model of the medium-power dry-type electrical transformer. Int J Therm Sci 2008. https://doi.org/10.1016/j.ijthermalsci.2007.11.004.

[62] Ahn HM, Lee BJ, Hahn SC. An efficient investigation of coupled electromagnetic-thermal-fluid numerical model for temperature rise prediction of power transformer. 2011 Int. Conf. Electr. Mach. Syst. ICEMS 2011, 2011. https://doi.org/10.1109/ICEMS.2011.6073995.

[63] Liao C, Ruan J, Liu C, Wen W, Du Z. 3-D coupled electromagnetic-fluid-thermal analysis of oil-immersed triangular wound core transformer. IEEE Trans Magn 2014. https://doi.org/10.1109/TMAG.2014.2330953.

[64] Ahn HM, Kim JK, Oh YH, Song KD, Hahn SC. Multi-physics analysis for temperature rise prediction of power transformer. J Electr Eng Technol 2014. https://doi.org/10.5370/JEET.2014.9.1.114.

[65] American Society of Heating Refrigerating and Air-Conditioning Engineers Inc. ASHRAE Handbook: Refrigeration (SI Edition). 2010.

AUTHORS PROFILES

KENDEG ONLA Clement junior was born in Mbongo-Ndonga in Cameroon, on February 11, 1994. He received the B.Eng. degree in electrical engineering from Higher Institute of Technology and Industrial Design, Douala, Cameroon, in 2015 and the M.Sc. degree in Electronics, Electrical Engineering and Automation (EEA) from Ngaoundere University, Cameroon, in 2018.

He is currently work toward the Ph.D. degree in electrical machines design, modeling, control and optimization at the University of Ngaoundere, Cameroon.

His research interests include electrical machines and drives for renewable energy power generation, electrical transformers and electromagnetic devices modeling.

KENMOE FANKEM Eric Duckler received the M. Sc degree in Electrical Engineering and Electronics from the National Polytechnic School of Lorraine, Nancy, France in

2007 and the Ph. D. degree in Electrical Engineering in 2012, from the University of Lorraine, Nancy, France.

He is currently Senior Lecturer in the Department of Physics of the Faculty of Science of the University of Ngaoundéré, Cameroon. His main lectures are related to Electrical machines, power converters, automation and control systems.

His fields of interest are design, modelling and control of special machines, electrical transformers, power converters and energy systems.

DOUNTIO TCHIOFFO Alix received the B. Sc. and M.Sc degrees in Electronics, Electrical Engineering and Automation from the Department of Physics of the University of Ngaoundéré, Cameroon respectively in 2008 and 2013.

His current work toward the Ph.D. degree in Electrical Engineering at the same University is focussed on the control Brushless Doubly-Fed Induction Generator.

His interests in research are related to renewable energy systems, electrical machines modelling / control.

Effa Joseph Yves received his PhD in Electronics from the University of Yaounde I, Cameroon. He is Currently Professor in Electronics at Department of Physics from the University of Ngaoundere, Cameroon.

He is author and co-author of more than 30 publications in prestigious journals and conferences and he is Reviewer for various international journals.He has more than 14 years' experience of education and research and he supervised more than 40 Master's degree students and 4 PhD students.

His research interests include chaos detection, synchronization of chaotic systems, nonlinear transmission line, Signal Processing and Image Processing, chaos-based image encryption and renewable energy.